Journal of the European Ceramic Society 20 (2000) 1053–1060

New evidence for an oxycarbonate phase as an intermediate step in $BaTiO_3$ preparation

S. Gablenz [a], H.-P. Abicht [a,*], E. Pippel [b], O. Lichtenberger [b], J. Woltersdorf [b]

[a] *Martin-Luther-Universität Halle-Wittenberg, Fachbereich Chemie, Kurt-Mothes-Str. 2, D-06120 Halle, Germany*
[b] *Max-Planck-Institut für Mikrostrukturphysik Halle, Weinberg 2, D-06120 Halle, Germany*

Received 22 April 1999; received in revised form 25 August 1999; accepted 12 September 1999

Abstract

A newly developed method of spray hydrolysis of a barium-titanium double alkoxide will be described as an efficient synthetic route for the preparation of a stoichiometric $BaTiO_3$ powder. During the thermal treatment of the corresponding precursor a barium-titanium oxycarbonate appears as an intermediate. High resolution electron microscopy (HREM) and electron energy loss spectroscopy (EELS) at ionization edges (ELNES), along with X-ray powder diffractometry (XRD), Fourier-transformed infrared spectroscopy (FTIR), and thermoanalytical measurements provide evidence of the existence of such an oxycarbonate phase. The comparison of the measured EEL spectra with quantum-mechanical calculations using density functional theory (DFT) reveals that this intermediate phase is characterized by an electronic C-Ti interaction in the crystal lattice and a specific modification of the carbonate bond.

Keywords: Barium titanium oxycarbonate; $BaTiO_3$; Calcination; Powders-chemical preparation; Spray hydrolysis

Zusammenfassung

Eine neu entwickelte Methode der Sprühhydrolyse eines Barium-Titan-Doppelalkoxids wird als effizientes Syntheseverfahren zur Herstellung eines stöchiometrischen $BaTiO_3$-Pulvers beschrieben. Im Verlaufe der thermischen Behandlung des entsprechenden Precursors bildet sich eine Barium-Titan-Carbonatoxid-Zwischenphase: Hochauflösende Elektronenmikroskopie (HREM), Elektronenenergieverlustspektroskopie (EELS) in Ionisationskantennähe (ELNES), in Verbindung mit Röntgenpulverdiffratometrie (XRD), Fourier-transformierter Infrarotspektroskopie (FTIR) und thermoanalytischen Messungen beweisen die Existenz der Carbonatoxid-Phase. Der Vergleich der gemessenen EEL-Spektren mit quantenmechanischen Berechnungen unter Verwendung der Dichtefunktionaltheorie (DFT) ergibt, daß diese Zwischenphase gekennzeichnet ist durch eine elektronische C-Ti-Wechselwirkung im Kristallgitter und eine spezielle Modifikation der Carbonatbindung.

1. Introduction

The classical mixed oxide method[1] is widely used for the preparation of $BaTiO_3$-based PTC (positive temperature coefficient of resistivity) ceramics. Particularly inhomogeneities of the stoichiometry caused by the incomplete mixing and leaching of Ba^{2+} ions from surface-near layers during the wet milling of calcined $BaTiO_3$ powders[2] speeded up the development of alternative synthesis procedures to a larger extent. Consequently, selected coprecipitation techniques,[3] hydrothermal methods,[4] the thermal decomposition of precursors[5,6] as well as special sol gel procedures[7–12] as the methods for the $BaTiO_3$ synthesis have evolved during the last three decades.

One of the most important precursor methods to produce stoichiometric $BaTiO_3$ is the oxalat method.[5] $BaTiO_3$ powders prepared after this method stand out against others due to their exact atomic [Ba/Ti] ratio of 1, on the one hand, but they are associated with the formation of coarse and hard agglomerates ($\leqslant 400$ μm) that is difficult to control, on the other.

A sol gel method frequently used is the Pechini method.[7] The $BaTiO_3$ powders obtained consist of particles with

* Corresponding author.
E-mail address: abicht@chemie.uni-halle.de (H.-P. Abicht).

0955-2219/00/$ - see front matter
PII: S0955-2219(99)00242-3

very small diameters of about 30 nm and a relatively narrow grain size distribution. However, using an excess of barium as described below makes clear, that it is problematic to adjust the exact [Ba/Ti] stoichiometry via this method. Using the recently developed method of spray hydrolysis of a barium titanium double alkoxide described in this paper allows one to produce fine-grained $BaTiO_3$ powders with a relatively narrow grain size distribution and an exact [Ba/Ti] stoichiometry.

The above methods have in common, that during the thermolysis of the precursors an intermediate product occurs in the temperature range between 500 and 600°C. The true nature of this species[5–12] has been discussed controversially up to now. The powders all show the same diffuse signals in their X-ray powder diffractograms and have a gross composition of $Ba_2Ti_2O_5CO_3$. This interphase seems to function as a key component in the course of the genesis of $BaTiO_3$ powder derived from organic precursors. The existence of such an oxycarbonate-like interphase was pointed out first by Gopalagrishnamurthy et al.[5] who studied the thermolysis of barium titanyl oxalate. In their thermal gravimetric analyses the authors observed the formation of a metastable phase with the gross composition of $Ba_2Ti_2O_5CO_3$. The diffuse X-ray powder diffractogram could not be assigned to any known substance. Vasyl'kiv et al.[6] have doubted the existence of the intermediate phase as a pure compound. They describe the nature of the phase as a mixture of amorphous TiO_2, BaO and $BaCO_3$. Hennings et al.[8] describe the interphase as a mixture of $BaCO_3$ and TiO_2 in finest distribution. Kumar et al.[9] assign the X-ray powder diffractogram obviously to the phase $Ba_2Ti_2O_5CO_3$. From X-ray photoelectron spectroscopy results Cho[10] concluded, that the interphase is not a barium titanium oxycarbonate but hexagonal $BaTiO_3$ stabilized with Ti^{3+} ions. In their recently published work, Tsay et al.[11] describe the metastable phase as a structure of $BaTiO_3$ with carbonate ions deposited on the barium titanate layers. In preparing $SrTiO_3$ via the Pechini method Leite et al.[12] succeeded in evidencing the existence of an adequate interphase of the gross composition $Sr_2Ti_2O_5CO_3$. Also in this case there was an X-ray powder diffractogram which could not be assigned to any known crystalline phase.

The present paper first of all describes the synthesis of $BaTiO_3$ powders by the newly developed spray hydrolysis method. Then some new investigations connected with the existence of the barium titanium oxycarbonate interphase are pointed out during the thermal evolution of crystalline $BaTiO_3$.

Differential thermoanalysis and thermogravimetry (DTA/TG), high resolution transmission electron microscopy (HRTEM), electron diffraction and electron energy loss spectroscopy (EELS), especially the analyses of near-edge structures (ELNES) were used as analytical methods. The interpretation of the measured ELNES of the different phases required quantum-mechanical calculations to be performed using the Density Functional Theory (DFT). Comparative investigations followed of heat-treated samples of powders prepared by spray hydrolysis and by the oxalate method, respectively, applying X-ray powder diffraction (XRD) and Fourier transformed infrared spectroscopy (FTIR).

2. Materials and methods

A conventional barium titanium double alkoxide (BTD) (ABCR GmbH & Co.) was used as a well hydrolyzable organometallic precursor. The hydrolysis process was performed using a modified mini spray drier Büchi B-191 (Büchi GmbH) according to Fig. 1.[13] A pump transports the BTD to the spray nozzle (diameter = 0.7 mm). Argon as an inert gas is used to prevent undesirable hydrolysis to occur. The spray nozzle is connected to compressed air (600 l h^{-1}). The BTD is sprayed into the spray cylinder and hydrolyzed by a preheated (180°C) steam/air mixture (35 m^3 h^{-1}) that is sucked in by an aspirator. In order to ensure a complete reaction, a water/BTD molar ratio >14 was maintained during the spray hydrolysis process. The as-prepared powder was separated by a cyclone.

The barium titanyl oxalate (BTO) was prepared following Clabaugh et al.[14] using $TiCl_4$, BaC_2O_4 and $H_2C_2O_4$ (Merck, p. A.) as starting materials. Both precursor powders were heat-treated in air in the chamber

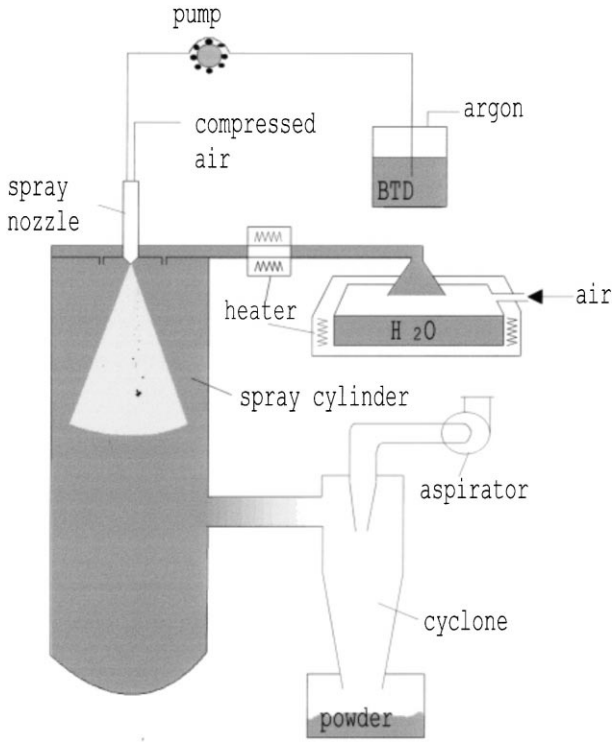

Fig. 1. The spray hydrolysis equipment used.

furnace CSF 1200 (Carbolite) at temperatures given below for 1 h, using a heating rate of 10 K min^{-1}. To determine the atomic [Ba]/[Ti] ratio 300 mg of the appropriate sample were dissolved in a mixture of 2 ml $HClO_4$ (Riedel-De Haen AG, p. A.) and 20 ml H_2O_2 (Merck p.A.) at 50°C. The content of titanium was determined via complexometric titration and that of barium was determined gravimetrically as $BaSO_4$.[15] The average particle size and its distribution were analysed using the particle size analyser SA-CP3 (Shimadzu). Changes in structure and formation of the crystalline phases were monitored by X-ray powder diffraction (XRD) which was performed by using a URD 63 diffractometer (Freiberger Präzisionsmechanik GmbH) with Cu-K_α radiation ($\lambda = 154.05$ pm) in the range $2\Theta = 20–55°$ (Θ — Bragg angle) with a resolution of $\Delta 2\Theta = 0.05°$. Thermoanalytic investigations were performed in air at temperatures between 20 and 1100°C with a heating rate of 10 K min^{-1} using the STA 409 C (Netzsch). The Fourier transformed infrared spectra were collected for disk specimens mixed with KBr using a Mattson 5000 spectrometer (Mattson Instruments Inc.).

The interesting peculiarities concerning the microstructure and nanochemistry of the barium titanium oxycarbonate intermediate phase were investigated by high resolution electron microscopy (HREM) and electron energy loss spectroscopy (EELS), especially on near-edge fine structures (ELNES). EELS was performed with an energy resolution of 0.8–1 eV using the Gatan imaging filter (GIF 200) attached to the transmission (TEM)/scanning transmission electron microscope (STEM) Philips CM 20 FEG operated at 200 keV. Point analyses were made in the nanoprobe mode with the electron probe of a few nanometres in diameter. For spectrum processing the software packages Digital Micrograph and EL/P of Gatan were used. For the TEM investigations, specimens of the powders calcined at 600°C were prepared by dispersing a small amount of the powder in pure alcohol, mixing it in an ultrasonic generator, and pipetting a drop of this dispersion on a copper mesh covered with a holey Formvar film. To compare the ELNES features with those of the intermediate phase specimens of $BaCO_3$ powder were also prepared.

To minimize the contamination effects during the analyses, which are generally strong for electron probes as small as some nanometres, the specimen grid was kept at the liquid-nitrogen temperature via a cooling specimen holder (Gatan model 668). In order to simulate the onset of the measured C-K ELNES as well as the number of peaks and their experimentally observed energies, quantum-mechanical calculations have been performed using the Density Functional Theory (DFT). The gradient corrected exchange functional proposed by Becke[16] and the correlation functional by Perdew[17] have been used to calculate the total energies and gradients and the energy eigenvalues of the electron levels. For the calculation of the electronic structure of compounds including transition metal atoms, correlation effects as backbonding have to be considered. Therefore, for our DFT calculations a DN* basis set has been chosen (double numerical with polarization functions), i.e. one function for the core orbitals (O- and C-1s, 2s, 2p, 3s, 3p), two functions for valence ortitals (O- and C-2s, 2p, Ti-4s, 3d) and one function for unoccupied C- and O-3d orbitals, respectively. Functions of higher angular quantum number than are formally occupied in the atom in its ground state are required for the inclusion of the backbonding effect. To characterize the newly found oxycarbonate phase, the well-known ordinary carbonate (represented by the cluster in Fig. 2(a)) has been compared with a cluster representing the assumed oxycarbonate phase in a short-range order (Fig. 2(b), derived from a proposal of Louër et al.[18]). Both these clusters have been used for the DFT calculations.

3. Results and discussion

To make sure that the calcination of the precursor prepared via spray hydrolysis does not modify the atomic [Ba]/[Ti] ratio both the as-prepared powder and that heat-treated at 1100°C for 2 h were chemically analyzed. The atomic ratio was $[Ba/Ti] = 1.0007 \pm 0.0001$. Therefore, neither the contact of the powder with water during the spray hydrolysis nor the calcination process, which is necessary to eliminate the remaining organic residue, causes a change in the chemical composition. The atomic [Ba]/[Ti] ratio remains constant according to the initial setting-up given by the nature of the molecular barium titanium double alkoxide.

The particle size analysis showed that the powder prepared by the spray hydrolysis and heat-treated at 1100°C for 1 h consists of particles with an average diameter of 1.28 μm. Fig. 3. illustrates the particle size distribution of the powder. Obviously, for 85% of the particles the diameter varies between 1 and 1.5 μm.

In order to prove the suitability of the as-received barium titanate as a starting powder for the preparation

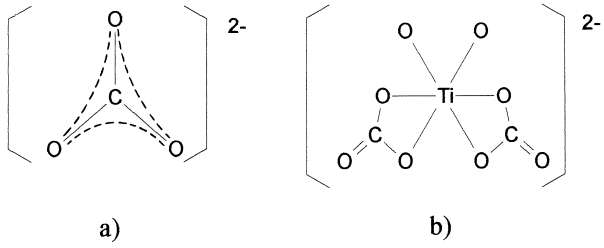

Fig. 2. Clusters for the calculation of energy eigenvalues using DFT. (a) Carbonate phase; (b) oxycarbonate phase.

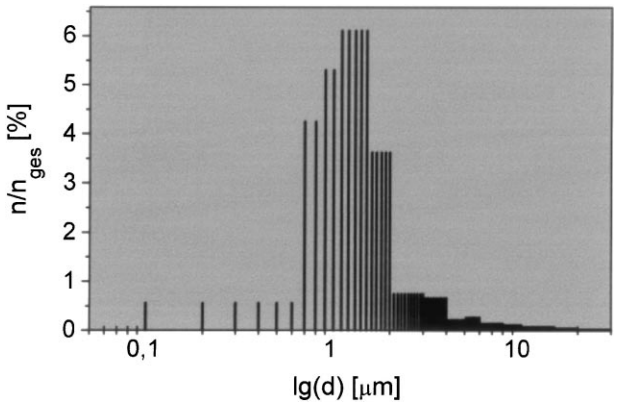

Fig. 3. Particle size distribution of the powder prepared by spray hydrolysis and calcined at 1100°C for 1 h (d — particle diameter; n — number of particles with certain diameter; n_{ges} — overall number of particles).

of ceramics the calcined powder was pressed into cylindrical disks (diameter 1.213 cm; height 0.255 cm) with a density of $d = 3.05$ g cm^{-3}, and then sintered at 1350°C for 1 h. The light-brown sintered bodies had a density of $d = 5.93$ g cm^{-3} corresponding to 98.63% of the theoretical density of $BaTiO_3$ single crystals ($d = 6.012$ g cm^{-3}).[19] The micrograph of Fig. 4, taken in reflected light, illustrates the untreated surface of an as-sintered specimen. The ceramics are characterized by a homogeneous grain structure, with an average grain diameter of 43 μm determined by the linear intercept technique of Saltykov.[20] An additional advantage of the $BaTiO_3$ powder prepared via spray hydrolysis is the fact that no pressing aids as well as homogenizing steps are necessary.

3.1. X-ray powder diffraction

X-ray powder diffraction was applied to evaluate the structural evolution of the barium titanate prepared by spray hydrolysis from the as-prepared powder to crystalline $BaTiO_3$. Fig. 5 shows the XRD pattern of six samples heat-treated for 1 h at different temperatures. It is obviously that both the as-prepared powder and the one heat-treated up to 400°C do not show any crystalline structure. The XRD pattern of the sample heat-treated at 600°C cannot be assigned to any known compounds cited in the JCPDS (Joint Committee of Powder Diffraction Standards) data file. There are, however, similarities to the XRD patterns published by the above-quoted authors.[8–11] The diffuse patterns with weak intensive peaks have been discussed controversially and have partly been assigned to a barium titanium oxycarbonate phase. As hardly any of these publications present the exact 2Θ values of the main signals, a direct comparison is impossible. Therefore, we examined a powder prepared via the oxalate method and heat-treated at 600°C by means of XRD. The most intensive XRD peaks of samples C (spray hydrolysis derived) and F (oxalate method) coincide with respect to the 2Θ values and the relative intensities of their signals. The most intensive peak in both spectra appears at $2\Theta = 26.6°$. Additional corresponding peaks occur at $2\Theta = 21.6°$; 34.3°; 43.2° and 44.2°, respectively. The pattern of the powder obtained by spray hydrolysis and heat-treated at 800°C (Fig. 5D) shows the typical peaks of cubic $BaTiO_3$[21] [$2\Theta = 21.9°$ (100); 31.3° (110); 38.6° (111) and 44.9° (200)] and traces of orthorhombic $BaCO_3$[22] [$2\Theta = 23.8°$ (111) and 24.2° (102)].

Heat-treating at 1100°C (Fig. 5E) results in the elimination of these carbonate traces and causes the

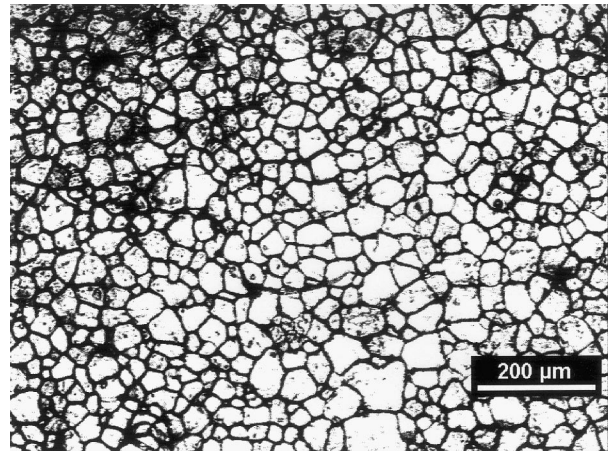

Fig. 4. Microstructure of a ceramics sintered at 1350°C for 1 h, prepared by spray hydrolysis.

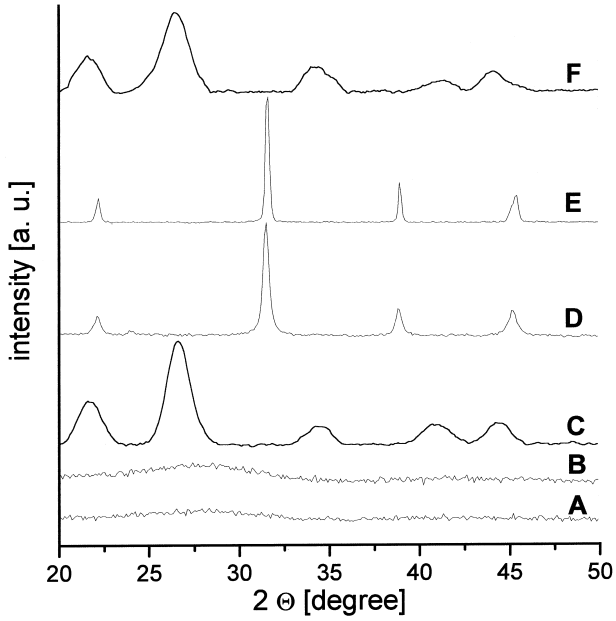

Fig. 5. X-ray powder diffraction pattern of powders prepared by spray hydrolysis (A to E) and by the oxalat method (F), calcined at various temperatures for 1 h (A: as prepared; B: 400°C; C: 600°C; D: 800°C; E: 1100°C; F: 600°C).

formation of tetragonal $BaTiO_3$.[19] The tetragonal splitting of the (200) peak indicates the phase transition from cubic to tetragonal $BaTiO_3$.

3.2. Differential thermoanalysis and thermogravimetry

Fig. 6 shows the TG and DTA curves of a powder obtained by spray hydrolysis. The weight loss at temperatures between 20 and about 450°C has to be attributed to the loss of water and organic species in the precursor powder due to the incomplete hydrolysis of barium titanium double alkoxide and insufficient drying, respectively. The two exothermic effects at about 320 and 420°C are due to the oxidative decomposition of organic species. The gain in weight at about 520°C correlates with an intensive exothermic effect and can be explained on the assumption that fixed low valent carbon is completely oxidized, remaining as carbonate within the material.

3.3. Fourier transformed infrared spectroscopy

The formation of the above-described carbonate species is supported by the typical XRD patterns on the one hand and by the FTIR spectra shown in Fig. 7. on the other. The FTIR spectra of the samples heat-treated at 400, 600 and 800°C seem to show the typical vibration modes of orthorhombic $BaCO_3$. The closer examination of the individual peaks showed that the energy position of the out-of-plane vibration of the carbonate ions changed in a characteristic way. The excitation frequency for this vibration mode is shifted from 857 cm^{-1}, typical of orthorhombic $BaCO_3$,[23] to 875 cm^{-1} for the sample heat-treated at 600°C (Fig. 7A; Table 1). This corresponds to a difference of about 18 cm^{-1} in the wave numbers. The other vibration modes are not shifted and correspond to those of orthorhombic $BaCO_3$ (Table 1). The observed shift is due to a change of the chemical or structural environment of the carbonate ions. Why is, however, only this single vibration type influenced?

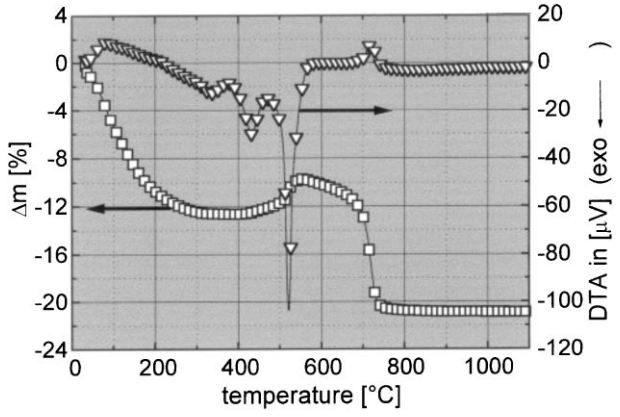

Fig. 6. DTA/TG measurements of a powder prepared by spray hydrolysis.

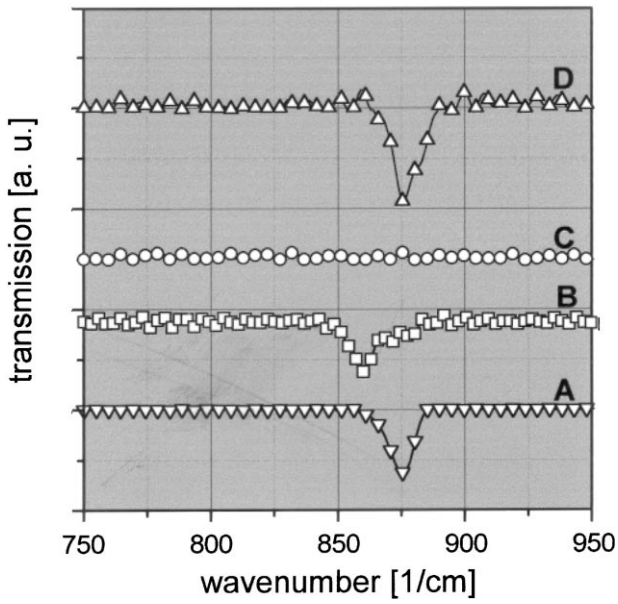

Fig. 7. FTIR spectra of powders prepared by spray hydrolysis (A to C) and by the oxalat method (D) calcined at various temperatures for 1 h (A: 600°C; B: 800°C; C: 1100°C; D: 600°C).

Comparing the FTIR spectra of homologous series of orthorhombic alkaline earth carbonates (Table 1) proves that unlike all the other vibrations the out-of-plane vibration remains constant with regard to its energetic position. If the crystallographic environment of the carbonate ions changes from the orthorhombic system of aragonite to the trigonal system of calcite, then the excitation energy of the out-of-plane vibration shifts to higher values like for the oxycarbonate phase. The excitation energy of the out-of-plane vibration therefore is influenced merely by the nature of the structural arrangement of the carbonate ions in the crystal. That means:

(i) the carbonate ions are components of a well-defined crystalline structure;
(ii) this crystalline structure does not correspond to orthorhombic $BaCO_3$.

The FTIR spectrum of the spray-hydrolyzed sample heat-treated at 800°C for 1 h (Fig. 7B) shows the signals of orthorhombic $BaCO_3$, which do not appear in the spectrum of the sample heat-treated at 1100°C for 1 h (Fig. 7C). This is in agreement with the corresponding XRD pattern shown above. One can assume that after decomposition of the oxycarbonate phase at temperatures between 600 and 800°C small amounts of carbonate traces probably remain in the surface-near layers.

The FTIR spectrum of the powder prepared by the oxalate method and heat-treated at 600°C for 1 h shows a shift in the excitation energy of the out-of-plane

Table 1
Wave number of vibration modes of the CO_3^{2-} ion in alkaline earth carbonates[20] and barium titanium oxycarbonate derived from spray-hydrolysed barium titanium double alkoxide (SPH) and from barium titanyl oxalate (BTO), both calcined for 1 h at 600°C

Powder	Modification	Crystal symmetry	δ_{ip}[a]	δ_{oop}[b]	ν_s[c]	$\nu_s + \delta_{ip}$
SPH/600°C/1 h			693	875	1059	1750
BTO/600°C/1 h			693	875	1059	1750
$BaCO_3$	Witherite	Orthorhombic	693	857	1059	1750
$SrCO_3$	Strontianite	Orthorhombic	702	856	1071	1774
$CaCO_3$	Aragonite	Orthorhombic	712	853	1082	1801
	Calcite	Trigonal	712	875	Inactive	1800

[a] In-plane vibration.
[b] Out-of-plane vibration.
[c] Symetric stretch vibration.

vibration of the carbonate ions. Corresponding to the respective heat-treated powder prepared by spray hydrolysis the shift amounts to about 18 cm^{-1} (Fig. 7D; Table 1). The FTIR spectra along with the characteristic XRD patterns give rise to the assumption that there is a discrete barium titanium oxycarbonate.

3.4. High resolution electron microscopy

From the broad maxima in the X-ray pattern of Fig. 5 (curves C and F) it can be concluded that the intermediate barium titanium oxycarbonate phase should consist of very small crystallites. To prove this, HREM investigations of these materials were performed. Fig. 8. shows a typical lattice plane image of an oxycarbonate specimen with irregularly arranged crystallites of approximately 4 nm in diameter. As indicated in this figure, the lattice plane distances were about 0.42 and 0.34 nm corresponding well to the two large maxima in the X-ray pattern, viz. $2\Theta = 21.6°$ (0.411 nm), and $2\Theta = 26.6°$ (0.334 nm). Similarly the intensity distribution of the broad rings in the electron diffraction pattern, incorporated in Fig. 8, corresponds to the X-ray pattern of Fig. 5.

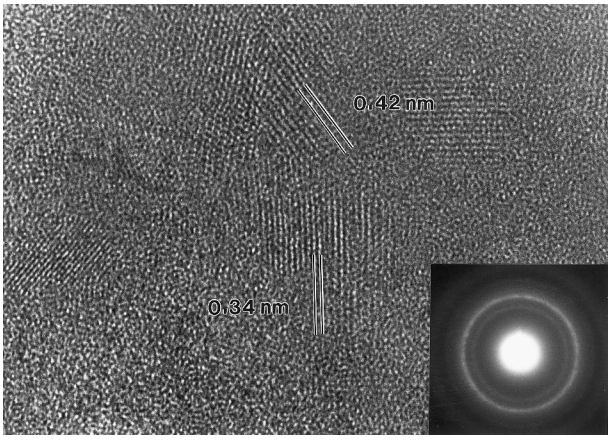

Fig. 8. HREM image of the barium titanium oxycarbonate intermediate phase (insert: electron diffraction pattern).

The above findings reveal that the barium titanium oxycarbonates produced via the spray hydrolysis and the oxalate method form a homogeneous nanocrystalline phase.

3.5. Electron energy loss spectroscopy and DFT calculations

In order to interpret the measured ELNES of the different phases and to explain the differences in their electronic structures a comparison is made between the experimentally obtained ELNES and the DFT calculations. As mentioned in Section 2, the DN* basis set has been used in order to include correlation effects. This leads to some hundred energy levels even for simple clusters.

Therefore, only the energy levels needed for the interpretation of the measured C-K ELNES are considered in the following.

For the cluster of the well-known carbonate (Fig. 2(a)), a C 1s level of 260.2 eV below the Fermi energy and a LUMO (lowest unoccupied molecular orbital) of +13.5 eV is obtained with mainly *p*-like atomic orbitals localized at both C and O atoms above the Fermi level (Fig. 9a).

Thus, a 1s $\rightarrow \pi^*$ peak in the C-K ELNES is expected at 273.7 eV. The measured EEL spectrum of the C-K edge shows the features typical of carbonates, viz. one marked 1s $\rightarrow \pi^*$ peak at about 290 eV, and a second broad peak at about 300 eV (Fig. 10(a)). The first peak is related to the calculated one. (Of course, the energy position of the experimentally measured peak in the ELNES cannot be reproduced exactly by DFT calculations, as the size and shape of the clusters chosen represent only a rough approximation of the real crystalline configuration. Moreover, the influence of the barium ions is neglected in the calculations.) The second peak can be interpreted as an inner well resonance,[24] being a many-electron excitation, which cannot be described by DFT models. For the oxycarbonate intermediate phase, represented by the cluster in Fig. 2(b),

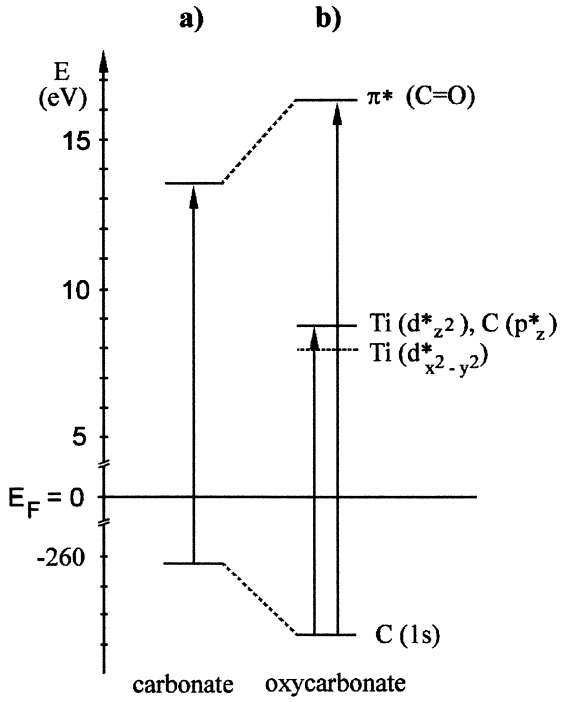

Fig. 9. Energies of the C 1s core level and the first unoccupied levels for the carbonate (a) and oxycarbonate (b) phase, respectively.

the calculations reveal additional features and a shift of the 1s $\rightarrow$ π^* peak. On the one hand, the C 1s level is shifted to 262.6 eV below the Fermi level, and on the other hand, the above-described molecular orbital consisting of O and C *p*-like atomic orbitals (representing the LUMO for carbonate) is shifted to 16.3 eV above the Fermi level. In addition, unoccupied molecular orbitals with titanium d-states participating occur at 7.9 (Ti-d_{x2-y2}) and 8.7 eV (mixed Ti-d_z2 and C-p) above E_F. These results (shown in Fig. 9(b)) are qualitatively in good agreement with the experimentally observed C-K ELNES of the oxycarbonate intermediate phase (cf. Fig 10(b)):

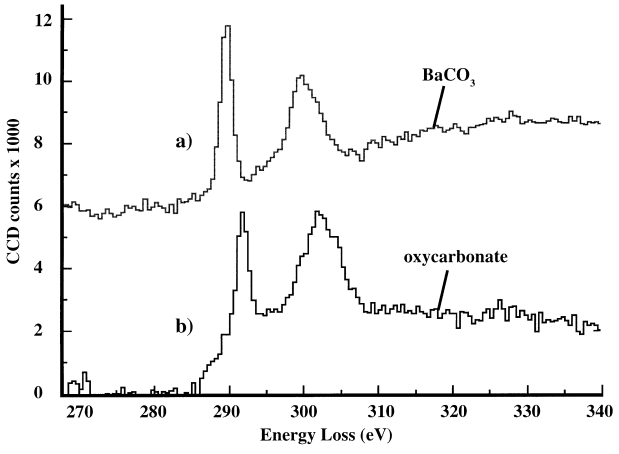

Fig. 10. Measured C-K ELNES of barium carbonate (a) and the barium titanium oxycarbonate intermediate phase (b).

the 1s $\rightarrow$ π^* peak assigned to the carbonate bond is shifted in the experimental spectrum by about 1.5 eV to higher energies, whereas at about 288 eV there is an additional shoulder close to the onset of the edge. Therefore, an electronic interaction between carbon and titanium follows for this phase.

The onset shifting indicates that the special bonding state of this phase is characterized by a specific modification of the carbonate bond. The increased energy difference between the oxygen 1s level and the unoccupied π^* level (cf. Fig. 9(b)) can be attributed to an enhanced oxidic contribution. Thus the designation "oxycarbonate" for this phase seems to be reasonable.

4. Conclusions

The spray hydrolysis of barium titanium double alkoxide has proven an efficient method for the synthesis of a stoichiometric $BaTiO_3$. Despite the high calcination temperature the resulting $BaTiO_3$ powder is distinguished by particles with a medium diameter of 1–1.5 μm and a homogeneous size distribution. The processing to ceramic materials does not require any further procedure and leads to sintered bodies that are characterized by a grain structure which is homogeneously with a mean grain diameter of 43 μm.

During the thermal evolution of crystalline $BaTiO_3$ a metastable barium titanium oxycarbonate forms, the existence of which has given reason for a number of controversial discussions. Thermal analytical investigations have enabled us to observe the formation of this oxycarbonate phase in-situ for the first time which is revealed by a remarkable gain in weight due to the oxidation of carbon species. Analysing the appropriate XRD pattern and a specific shift in the wave numbers of the out-of-plane vibration of the carbonate ions in the FTIR spectrum it was concluded that this phase is a substance with a definite crystalline structure. Carbonate ions are components of this structure but they do not correspond to those present in orthorhombic $BaCO_3$.

HREM and EELS investigations combined with quantum-mechanical DFT calculations for the first time provided evidence of such a crystalline intermediate oxycarbonate phase. Using HREM this new phase could be shown to exhibit a homogeneous nanocrystalline structure with the imaged lattice plane distances corresponding well to the XRD results. The measured EELS spectra, especially the ELNES analyses, and corresponding DFT-calculations have proven the existence of a special titanium oxycarbonate phase, characterized (i) by an electronic interaction between carbon and titanium, and (ii) by a specific modification of the carbonate bond in the sense of an enhanced oxidic contribution.

Acknowledgements

The authors wish to thank the Deutsche Forschungsgemeinschaft and the Fonds der Chemischen Industrie for financial support of this work.

References

1. Bauer, A., Bühling, D., Gesemann, H.-J., Helke, G. and Schreckenbach, W., Technologie und Anwendung von Ferroelektrika, Akademische Verlagsgesellschaft, Leipzig, 1976.
2. Abicht, H.-P., Völtzke, D., Röder, A., Schneider, R. and Woltersdorf, J., The influence of the milling liquid on the properties of barium titanate powders and ceramics. *J. Mat. Chem.*, 1997, **7**, 487–492.
3. Mulder, B. J., Preparation of $BaTiO_3$ and other ceramic powder by coprecipitation of citrates in alcohol. *Ceram Bull.*, 1970, **49**, 990–993.
4. Urek, S. and Drofenik, M., The hydrothermal synthesis of $BaTiO_3$ fine particles from hydroxide-alkoxide precursors. *J. Eur. Ceram. Soc.*, 1998, **18**, 279–286.
5. Gopalakrishnamurthy, H. S., Rao, M. S. and Kutty, T. R. N., Thermal decomposition of titanyl oxalates-I: barium titanyl oxalate. *J. Inorg. Nucl. Chem.*, 1975, **37**, 891–898.
6. Vasyl'kiv, O. O., Ragulya, A. V. and Skorokhod, V. V., Synthesis and sintering of nanocrystalline barium titanate powder under nonisothermal conditions. II. Phase analysis of the decomposition products of barium titanyl-oxalate and the synthesis of barium titanate. *Powder Metallurgy and Metal Ceramics*, 1997, **36**, 277–282.
7. Pechini, M. P. US patent 3 330 697, 11 July 1967.
8. Hennings, D. and Mayr, W., Thermal decomposition of (Ba, Ti) citrates into barium titanate. *J. Solid State Chem.*, 1978, **26**, 329–338.
9. Kumar, S., Messing, G. L. and White, W. B., Metal organic resin derived barium titanate: I, Formation of barium titanium oxycarbonate intermediate. *J. Am. Ceram. Soc.*, 1993, **76**, 617–624.
10. Cho, W.-S., Structural evolution and characterization of $BaTiO_3$ nanoparticles synthesized from polymeric precursor. *J. Phys. Chem. Solids*, 998, **59**, 659–666.
11. Tsay, J.-D., Fang, T.-T., Gubiotti, T. A. and Ying, J. Y., Evolution of the formation of barium titanate in the citrate process: The effect of the pH and the molar ratio of barium ion and citric acid. *J. Mat. Sci.*, 1998, **33**, 3721–3727.
12. Leite, E. R., Sousa, C. M. G., Longo, E. and Varela, J. A., Influence of polymerization on the synthesis of $SrTiO_3$: Part I. Characteristics of the polymeric precursors and their thermal decomposition. *Ceramics International*, 1995, **21**, 143–152.
13. Gablenz, S., Völtzke, D., Abicht, H.-P. and Neumann-Zdralek, J., Preparation of fine powders via spray hydrolysis of titanium tetraisopropoxide. *J. Mat. Sci. Lett.*, 1998, **17**, 537–539.
14. Clabaugh, W. S., Swiggard, E. M. and Gilchrist, R., Preparation of barium titanyl oxalate tetrahydrate for conversion to barium titanate of high purity. *J. Res. Nat. Bur Stds.*, 1956, **56**, 289–291.
15. Doerfel, K. and Geyer, R. Analytikum. Deutscher Verlag für Grundstoffindustrie, Leipzig, 1987.
16. Becke, A. D., Density-functional exchange-energy approximation with correct asymptotic behaviour. *Phys. Rev. A*, 1988, **38**, 3089–3100.
17. Perdew, J. P., Density-functional approximation for the correlation energy of the inhomogeneous electron gas. *Phys. Rev. B*, 1986, **33**, 8822–8824.
18. Louër, M., Louër, D., Gotor, F. J. and Criado, J. M., Crystal structure of barium titanyl oxalate $BaTiO(C_2O_4)_2$ * $4{,}5H_2O$. *J. Solid State Chem.*, 1991, **92**, 565–572.
19. Evans, H. T., An X-ray diffraction study of tetragonal barium titanate. *Acta Cryst.*, 1961, **14**, 1019–1026.
20. Saltykov, S. A., Stereometrische metallographie. Deutscher Verlag für Grundstoffindustrie, Leipzig, 1974.
21. Megaw, H. D., Crystal structure of barium titanate. *Nature*, 1945, **155**, 484–485.
22. de Villiers, J. P. R., Crystal structures of aragonite, strontianite, and witherite. *American Mineralogist*, 1971, **56**, 758–766.
23. Nakamoto, K., *Infrared and Raman Spectra of Inorganic and Coordination Compounds*. John Wiley & Sons, USA, 1986.
24. Bianconi, A., Core excitations and inner well resonances in surface soft X-ray absorption (SSXA) spectra. *Surface Sci.*, 1979, **89**, 41–50.